

Differential regulation of the transcriptomic and secretomic landscape of sensor and effector functions of human airway epithelial cells

Roland Lehmann¹, Mario M Müller^{1,2}, Tilman E Klassert¹, Dominik Driesch³, Magdalena Stock¹, Anina Heinrich¹, Theresia Conrad^{1,4}, Christoph Moore¹, Uta K Schier¹, Reinhard Guthke⁴ and Hortense Slevogt¹

Protein secretion upon TLR, TNFR1, and IFNGR ligation in the human airways is considered to be central for the orchestration of pulmonary inflammatory and immune responses. In this study, we compared the gene expression and protein secretion profiles in response to specific stimulation of all expressed TLRs and in further comparison to TNFR1 and IFNGR in primary human airway epithelial cells. In addition to 22 cytokines, we observed the receptor-induced regulation of 571 genes and 1,012 secreted proteins. Further analysis revealed high similarities between the transcriptional TLR sensor and TNFR1 effector responses. However, secretome to transcriptome comparisons showed a broad receptor stimulation-dependent release of proteins that were not transcriptionally regulated. Many of these proteins are annotated to exosomes with associations to, for example, antigen presentation and wound-healing, or were identified as secretable proteins related to immune responses. Thus, we show a hitherto unrecognized scope of receptor-induced responses in airway epithelium, involving several additional functions for the immune response, exosomal communication and tissue homeostasis.

INTRODUCTION

The interaction of airway epithelial cells (ECs) with pathogens and endogenous signals play an important role in many acute and chronic lung diseases such as pneumonia, bronchial asthma and chronic obstructive lung disease (COPD). Epithelial cells express pattern recognition receptors (PRRs), integrate information from many receptors simultaneously, and bridge the innate and adaptive immune system cells through the release of chemokines and cytokines.¹ Although accumulating evidence suggests more comprehensive responses, data of the complete landscape of transcriptional regulation and protein secretion of epithelial cells has not yet been collected so far. However, a better understanding of normal and altered epithelial functions is needed to provide new insights into the pathophysiology of airway diseases and to identify new epithelial-targeted therapies.² Recently, disease-related secretomes of the airway system were investigated using proteomic

techniques, which revealed novel mechanisms and new therapeutic targets on a general biological systems level.^{3,4}

We analyzed the receptor-specific sensor and effector functions of airway ECs induced by the recognition of microbial-associated molecular patterns (MAMP) of microorganisms and by cytokines respectively using RNA sequencing and LC-MS/MS based proteomics. Toll-like receptors (TLR) constitute one of the best studied families of PRRs that play a critical role in the host defence of the respiratory tract as they recognize invading pathogens, such as bacteria, viruses and fungi leading to cell activation and inflammation.^{5,6} The repertoire for detecting particular MAMPs by the innate immune system is expanded by the cooperation between different TLRs.⁷ TLR2, for instance, associates with either TLR1 or TLR6 as heterodimer to facilitate recognition and induce signaling, and the activation of TLR4 by lipopolysaccharides (LPS) requires the presence of MD-2 and also CD14 and LBP

¹Septomics Research Centre, Jena University Hospital, Jena, Germany. ²Integrated Research and Treatment Centre - Centre for Sepsis Control and Care (CSCC), Jena University Hospital, Jena, Germany. ³BioControl Jena GmbH, Jena, Germany and ⁴Research Group Systems Biology and Bioinformatics, Leibniz Institute for Natural Product Research and Infection Biology - Hans Knoell Institute, Jena, Germany. Correspondence: H. Slevogt (hortense.slevogt@med.uni-jena.de)

Received 12 January 2017; accepted 17 October 2017; published online 3 January 2018; doi:10.1038/mi.2017.100

for the recognition of the smooth type of LPS.^{8,9} However, no comprehensive data are available regarding the cellular activation responses of these different receptor complexes. Furthermore, the actual TLR expression pattern in primary human airway ECs are still uncertain as divergent results have been reported for various airway epithelial cell lines and primary cells. Also, a thus far undetermined unresponsiveness of bronchial epithelium to LPS, despite the expression of TLR4, has been reported.^{10–14}

The focus of research so far has been the downstream signaling cascades of TLRs described to consist of highly overlapping signaling cascades that initiate the transcription and release of certain effector molecules, mainly cytokines and chemokines, that are involved in the activation and recruitment of professional immune cells.^{15,16} However, TLRs have also been reported to be involved in the regulation of cell migration, wound repair and proliferation in order to restore tissue homeostasis.^{17,18} Accordingly, an initial analysis of the overall secretome of TLR4-stimulated murine macrophages revealed 4,976 secreted proteins, of which 775 were upregulated, and showed a transcriptionally decoupled release of lysosomal proteins.¹⁹ These data suggest that TLR activation-dependent protein secretion includes many so far undescribed proteins taking part in the overall receptor response.

Airway ECs are also equipped with receptors to respond to cytokines. Thus, besides functioning as sensors of invading pathogens, airway ECs are also acting as effector cells of signals initiated by immune cells such as alveolar macrophages and lymphocytes.²⁰ In this study, we therefore also addressed the impact of tumor necrosis factor alpha (TNF α) and interferon gamma (IFN γ) that can be released by immune cells and have been demonstrated to play significant roles in most infectious and inflammatory pulmonary diseases, including lower respiratory tract infections, pulmonary tuberculosis (PTB), chronic bronchitis (CB), chronic obstructive pulmonary disease (COPD), bronchial asthma, and in acute respiratory distress syndrome (ARDS).^{21–23} TNF α is a cytokine primarily released by activated macrophages that, similarly to TLRs, induces signaling via the NF- κ B pathway to regulate pro-inflammatory responses, cell proliferation, differentiation, as well as cell survival and death. In contrast, the effector cytokine IFN γ is secreted predominantly by natural killer (NK) cells, natural killer T (NKT) cells and cytotoxic T lymphocytes (CTL) and acts, like intracellular TLRs, through interferon regulatory factors (IRF) to play a central role for innate and adaptive immunity against viral and intracellular infections and enhances cellular immune processes.

Here we provide a comprehensive investigation of the landscape concerning specific TLR-, TNFR1-, and IFNGR-mediated protein secretion of the airway epithelium by combining mass spectrometry-based secretome analyses with RNA sequencing data. The results of our study attributes proteins to new regulatory mechanisms of secretion and functions and reveals their regulation upon differential receptor stimulations. Our findings have the potential to contribute to

the development of new strategies to modulate mucosal immune responses in human airways.

RESULTS

Normal airway epithelial cell-specific receptor expression

We verified the presence of predominantly epithelial cells in our submerged primary cell cultures by flow cytometry analysis of markers expressed on epithelial cells (E-cadherin), club cells (CC10),²⁴ and fibroblasts (Vimentin) (**Supplementary Figure S1e** online). Furthermore, we characterized the expression of TLR 1–9, TNFR1/2 and IFNGR1/2 in our normal human bronchial epithelial cells (NHBE) at the transcript and protein level. The expression of TLR 1–6, TNFR1 and IFNGR1/2 was detectable by RT-PCR, whereas expression of TLR 7–9 and TNFR2 was not (**Figure 1a**). We further confirmed these results by re-analyzing our RNA sequencing data from subsequent experiments (**Figure 1a**, **Supplementary Table 2**). While IFNGR1 and 2 are mandatory for signaling as IFNGR, only TNFR1 is needed for signaling after ligation with TNF α . Moreover, using qRT-PCR, we assessed the expression kinetic of the receptors across the different stimulations for the whole duration of the experiment. Besides an increase of TLR2 and TLR3 expression by Poly I:C after 16 h, we found no substantial changes in receptor expression (**Supplementary Figure 2c**).

For protein level verification, we included a glycoproteome enrichment-based LC-MS/MS analysis of NHBE cell lysate. The analysis of the 5,281 identified proteins revealed 368 expressed receptors (GO: 0004872) and confirmed the expression of the TLRs 1–6, TNFR1 and IFNGR1/2 (**Figure 1a** and **Supplementary Table 2**). In addition, the TLR4 co-stimulators MD-2 and CD14 were detected at transcriptional, as well as protein expression level.

We analyzed the cellular activation response induced by each receptor-specific ligand with regard to their protein secretion and gene expression profiles using mass spectrometry and RNA sequencing, as outlined in **Figure 1b**. None of the stimulations with the indicated concentrations of ligands affected cell viability or the morphological appearance of the NHBE cell layer (**Supplementary Figure S1a–d**).

Highly similar gene expression induced by TLRs and TNFR1

The stimulation of TLR 1–6 is generally known to activate very similar intracellular signaling pathways that induce the expression of a confined set of similar genes involved in immune responses and inflammation.²⁵ In order for choosing the most relevant time point for the transcriptome analysis we performed a pilot study to investigate expression kinetics of immune relevant genes after PRR stimulation in NHBE cells. Six different cytokines (CXCL1, CXCL2, CXCL8, IL6, CCL20, and IL17C), that are known to be secreted and transcriptionally regulated by bronchial epithelium after TLR ligation, were analyzed at time points 2 h, 4 and 8 h post stimulation. We identified the overall highest transcriptional response after 4 h of stimulation (**Supplementary Figure S2a**), in accordance with comprehensive transcriptome data from previously

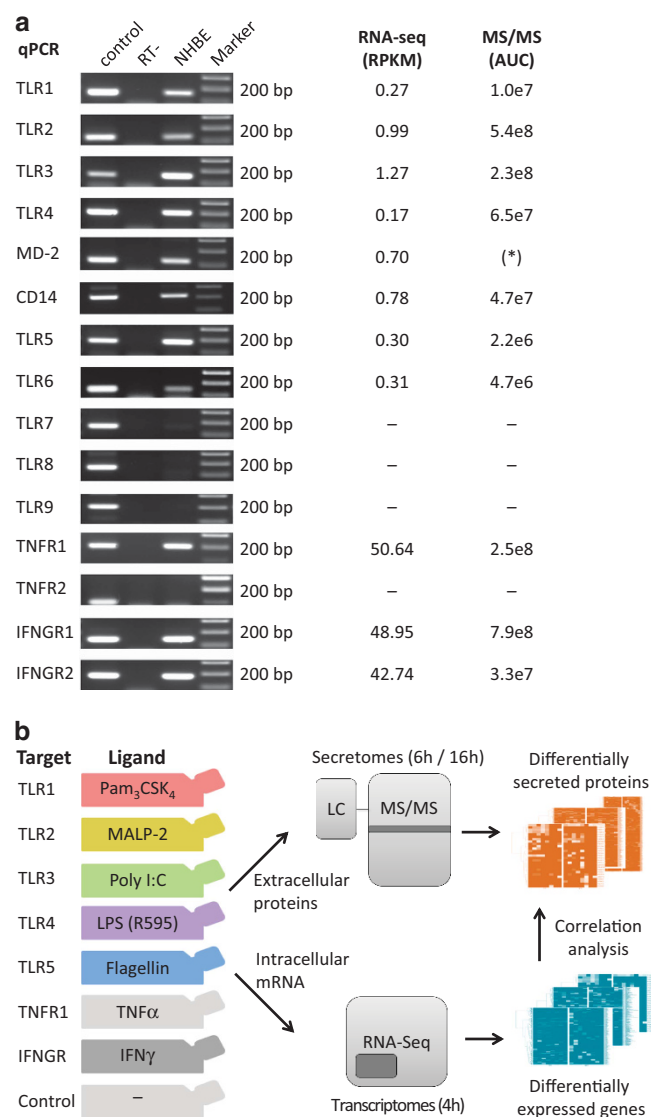


Figure 1 Receptor expression profile of airway ECs and experimental workflow. (a) Basal receptor gene expression was analyzed by RT-qPCR, RNA sequencing and glycoproteome based LC-MS/MS analysis (MS/MS). Peripheral blood mononuclear cells were used as positive control samples and are indicated as control. Negative control samples of RT-qPCRs without the addition of reverse transcriptase are marked with RT-. RNA sequencing results are shown as mean RPKM values from biological triplicates (threshold ≥ 0.1) (Supplementary Table 2 online). Receptor proteins were identified and quantified by mass spectrometry after glycoproteome isolation. Shown are the mean label-free quantified area under the curve values (AUC) obtained from of each receptor protein (Supplementary Table 2 online). MD-2 expression was confirmed by western blot (Supplementary Figure S1g online). (b) Schematic illustration of the experimental workflow for the analysis of the transcriptional and secretory response of airway ECs after specific receptor stimulations with the indicated ligands.

published studies with human airway epithelial cells²⁶ and murine macrophages.¹⁹

RNA sequencing at 4 h post receptor stimulation revealed 11,781 expressed genes (RPKM > 1) of which 552 were significantly upregulated and 19 downregulated (FC > 2) (Figure 2a and Supplementary Table 2). We observed a high overlap of regulated gene transcriptions induced by

receptor-specific ligands for TLR1/2 (Pam₃CSK₄), TLR2/6 (MALP-2), TLR3 (Poly I:C), TLR5 (Flagellin), but also with TNFR1 (TNF α), which contrasted with the transcriptional response of the IFNGR (IFN γ) stimulation. These findings were underlined by the respective mean fold change distances of expressed genes induced by each receptor ligand (Figure 2b). The distances of Poly I:C (TLR3) were less proximate to the other TLRs or TNFR1 agonists and closer to IFNGR (Figures 2a and b). Noticeably, LPS stimulation of primary airway ECs did not induce any significant change in gene expression (Figure 2a), which has also been observed in other studies.^{11,13,27} The largest and rather similar response was induced by TLR2/6 and TLR1/2, with 377 and 218 regulated genes respectively (Figure 2a), while the number of regulated genes for IFNGR was comparable, but with a very different profile.

The comparison of all differentially expressed genes from TLR ligand stimulations revealed a core set of 51 genes, that were equally regulated by all responding TLR stimulations, with further 21 genes solely not upregulated by the TLR3 ligand Poly I:C (Figure 2c). Many genes of this core set are not only encoding for cytokines and chemokines (e.g. *CCL5/20*, *CX3CL1*, *CXCL1/3/8*, *IL6*, *IL17C*, *IL23A*, *IL36G*), but also for genes with signal regulatory functions (*BIRC3*, *TNIP1*, *TNIP3*, *TNFSF15*, *IRAK2*), innate immune functions (*PTX3*) or antigen presentation and leucocyte adhesion (*CD83*, *OLR1*). We identified eight specifically upregulated genes by the TLR1/2 ligand Pam₃CSK₄, with associations to inflammation and haemato-regulatory functions (e.g. *DUSP1*, *CSF2*, *CXCL2*). Notably, with MIR3648 and MIR663A, we also found two specific regulatory microRNAs. The TLR3 ligand Poly I:C specifically regulated the expression of eight genes that encoded for proteins with antiviral properties (e.g., *IFIT1*, *IFIT2*, *IFIT3*, *ISG15*, *OASL*), which was further confirmed by a subsequent function enrichment analysis (Supplementary Figure S3a). Moreover, Poly I:C activated the expression of the IFN γ -inducible cytokines *CXCL9* and *CXCL11*.

Remarkably, TNF α induced the expression of 45 genes that belong to the TLR-ligand core set—not showing any discriminative gene expression on its own. This high degree of similarity is shown in Figure 2d. In contrast, the gene expression profile induced by IFN γ comprised 62 exclusively regulated genes, with specific functional associations to the complement system (*C1R*, *C1S*, *Serping1*) and antigen presentation (*HLA-E*, *TAP1*, *PSMB8/9*). Further enrichment analyses of GO-annotated biological processes for the shared gene expression profiles revealed predominantly processes related to various inflammatory immune responses (Supplementary Figure S3a). For the single ligand-specific regulated genes, we found functional enrichments for antiviral responses by Poly I:C and a type I interferon-associated response for the type II interferon (IFN γ) used here.

In addition, we investigated for cellular pathways that are linked to the differentially expressed genes of each receptor stimulation using a KOBAS (KEGG Orthology Based Annotation System) based analysis (Figure 2e). The results show that

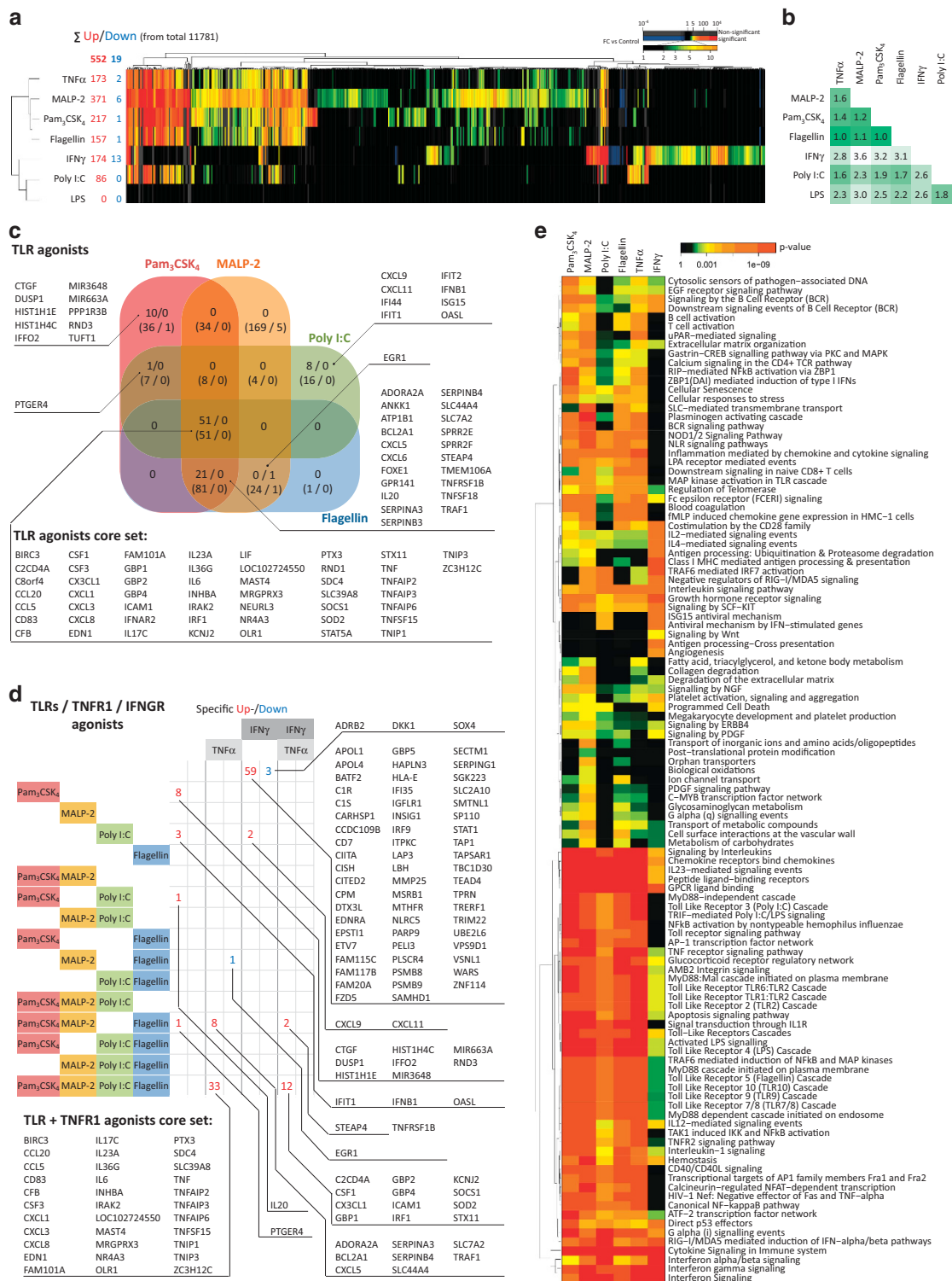


Figure 2 Transcriptome response profiles in response to receptor stimulation. **(a)** Hierarchical clustering of differentially expressed genes after 4 h of stimulation. Significantly regulated genes were grouped using unsupervised hierarchical clustering of fold-changes across the shown receptor stimulations. The fold changes of differentially expressed genes compared to control are colour-coded as indicated. Non-significant fold changes are coloured grey. All transcripts from biological triplicates with a FC > 2, a *P*-value < 0.05 and a mean RPKM value > 1 are displayed. **(b)** Table of normalized distances of mean fold changes between different stimulation responses of all expressed genes. Greater distances represent less similarity of gene expression patterns. **(c)** Venn diagram based overlap analysis of all responding Toll-like receptors showing the number of specifically regulated genes (up/down) distinctive for one TLR or several TLRs. Included are genes with a significant differential expression (*P*-value < 0.05) compared to all other stimulated receptor conditions. An overlap analysis testing differential expression only vs. the unstimulated control is shown in brackets. **(d)** Venn diagram overlap based table of all receptors, showing the number of regulated genes by one or several ligand stimulations after 4 h. **(e)** Pathway enrichment analysis based on the differential gene expression of each indicated receptor stimulation. Enrichment analysis was carried out using KOBAS including the databases of PID, BioCarta, Reactome and PANTHER, with a minimum enrichment *P*-value of 0.01 and an entity match of at least five genes per pathway, while generic pathway descriptions comprising more than 100 entities were excluded.

many cellular pathways are shared between TLR and TNFR1 ligand-based responses. These included several well-described signaling pathways, such as MyD88, TRIF and NF- κ B, but also several novel associations with pathways for hemostasis, extracellular matrix organization, G alpha signaling and apoptosis. Also notable for the stimulations by Pam₃CSK₄, MALP-2, Flagellin and IFN γ was the associated regulation of pathways involved in MHC-1-mediated antigen presentation and plasminogen cascade activation. Genes regulated by IFN γ and Poly I:C were both associated with antiviral responses, while IFN γ alone was linked to angiogenesis and Wnt signaling pathways.

Divergent protein secretion patterns between receptor stimulations

We analyzed the secretomes 6 and 16 h post stimulation to cover a generally recognized response peak of protein secretion and an early time point.^{19,28} The observed differential up- and downregulated protein secretion pattern shown in **Figure 3a** allow a comparison with the largely overlapping transcriptional response induced by these ligands as shown in **Figure 2a**. Our analysis revealed 4,830 identified proteins over all cellular supernatants, of which a total of 1,012 proteins were differentially secreted in response to the individual receptor ligands (**Figure 3a** and **Supplementary Table 2**). The hierarchical clustering showed specific patterns for each receptor stimulation and far less similarity of protein secretion compared to the results of the transcriptome responses (**Figure 2a**), with mean fold change distances from 2.7 to 4.9 (**Figure 3b**). We observed the highest number of differentially secreted proteins for Pam₃CSK₄ and IFN γ after 6h, caused also by a delayed and thus downregulated secretion of many proteins, which balanced after 16h. Therefore, and in accordance with other studies, we focused our further investigations on the 462 upregulated proteins.¹⁹ With up to 134 proteins, Pam₃CSK₄ and MALP-2 induced the highest, while LPS and Flagellin induced the lowest number of up to 58 differentially secreted proteins (**Figure 3a**). Besides a broad variety of receptor-specific proteins (**Supplementary Table 2**), we found that especially cytokines were commonly upregulated by two or more receptors (**Supplementary Figure S4a,b**). We analyzed all differentially released proteins in response to each receptor stimulation for biological processes and molecular functions using GO annotation enrichment at both time points (**Supplementary Figure S3b**). After 6 h of stimulation, we identified strong enrichments for GO terms related to cellular immune and defence mechanisms, such as inflammatory response for Pam₃CSK₄, response to molecules of bacterial origin for MALP-2 and Flagellin and leucocyte chemotaxis for Poly I:C. These enrichments were found to be predominantly associated with the secreted chemokines and cytokines. After 16 h, similar enrichments were found for the protein secretion profiles triggered by Flagellin, TNF α (leukocyte migration) and IFN γ (lymphocyte chemotaxis), whereas Pam₃CSK₄, MALP-2 and Poly-I:C now revealed a more heterogeneous enrichment

profile comprised of several metabolic processes or a “viral life cycle” association in the case of the TLR3 ligand Poly I:C. The response to LPS revealed a different profile, with “integrin-mediated adhesion” and “leucocyte migration” as notable enrichments after 16 h, but no enrichments related to inflammation or immune responses.

Receptor-induced transcriptionally independent protein release

While the transcriptional profiling of receptor activation revealed highly overlapping responses, the secretome of stimulated cells demonstrated higher variability in response to the different ligands and low transcriptional control. In order to attribute the secretome of airway ECs to the cellular source, we performed a GO annotation based cellular compartment enrichment analysis for all secreted proteins, where we found that the six highest enrichments were for compartments of extracellular vesicles and exosomes (**Figure 3c**). Further analysis revealed that up to 90% of the proteins associated with “extracellular region” were also annotated to the much smaller sub-term “extracellular exosomes” (**Figure 3d**). These proportions were principally valid for each investigated receptor stimulation, as shown by the similar ranges of cellular component associations for all analyzed secretomes (**Figure 3d**). Our findings were further supported by the ubiquitous presence of most of the top 25 exosomal marker proteins listed in ExoCarta - in addition to Muc1, Muc4, Muc16, as specifically described exosomal markers of human primary ECs in the secretomes (**Supplementary Figure S5**).^{29,30} For the receptor-specific analyses, we adopted the general secretome assignment scheme from (**Figure 3d**) in order to illustrate the cellular source, amount and transcriptional correlation of secreted proteins for each receptor ligand and time point (**Figure 3e**). The results confirm a large association to exosomes for each receptor-ligand-induced protein secretion. A high transcriptional overlap is observable for solely extracellular annotated proteins, with cytokines as the most prominent group of this fraction. Exosomal and other proteins were generally found far less likely to be transcriptionally regulated. This was especially noticeable for the transcriptionally independent secretion of proteins induced by LPS. The quantification of the exosome marker CD9 by ELISA confirmed the broad presence of around 10 ng ml⁻¹ exosomes in the secretomes of NHBE cells with no significant differences between stimulations (**Supplementary Figure S5b**).

Cytokines as dominant group for transcriptionally regulated protein secretions

A correlation analysis of receptor ligand-induced transcriptomes and secretomes showed a small amount of direct correlations at both time points (**Figure 4** and **Supplementary Table 2**). This indicates a considerable post-translational regulation for most secreted proteins in airway ECs. This is not attributable to cell leakage, as most transcriptionally upregulated genes were either not found or did not change their abundance in the respective secretomes after stimulation

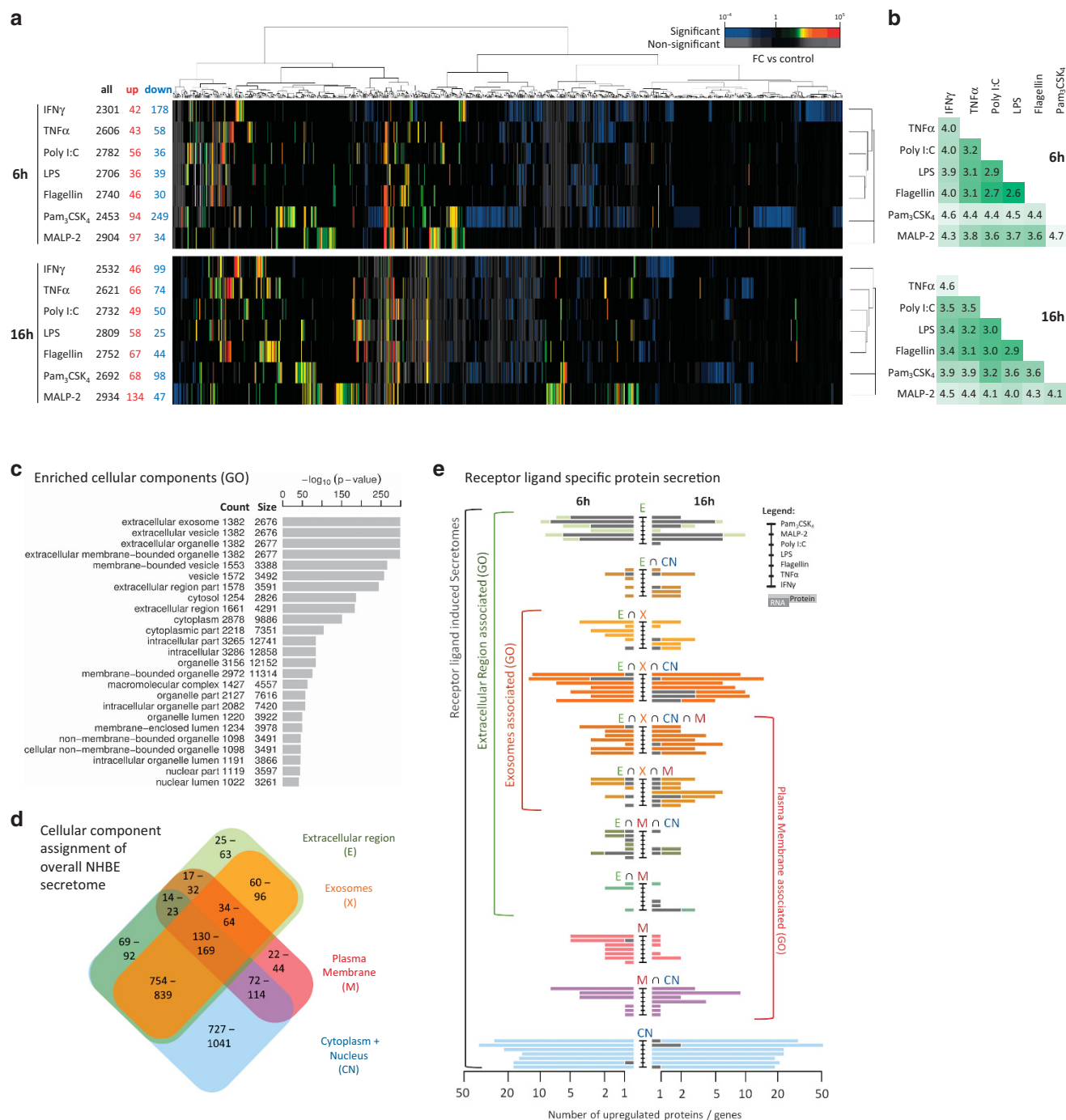


Figure 3 Secretome response profiles after receptor stimulation. **(a)** Identified proteins secreted 6 h and 16 h after receptor stimulation were grouped using unsupervised hierarchical clustering of fold changes across the indicated receptor stimulations. The fold changes of differentially secreted proteins compared to control are colour-coded as indicated. Non-significant fold changes are shaded in grey. Shown are the results from biological and technical triplicates with a minimum FC of 2 and a P -value < 0.05 . **(b)** Table of normalized mean fold change distances between different stimulation responses of all secreted proteins. Greater distances represent less similarity of protein secretion patterns. **(c)** GO enrichment analysis of cellular components of all identified proteins in the secretomes of NHBE cells for all stimulations. Shown are the 25 most significantly enriched cellular components with a minimum entity size > 500 . **(d)** GO annotation based Venn diagram depicting the overlap of major cellular component categories for all proteins identified after receptor stimulations. Different colours indicate different cellular compartments: green for extracellular region, brown for exosomes, red for plasma membrane and blue for cytoplasm and nucleus. **(e)** Receptor stimulation and time-specific distribution of proteins in accordance with the scheme of **Figure 3d**. The overlap of secretome and transcriptome regulations for differentially secreted proteins is superimposed in grey bars. The particular proteins can be found in **(Figure 5 and Supplementary Table 2 online)**.

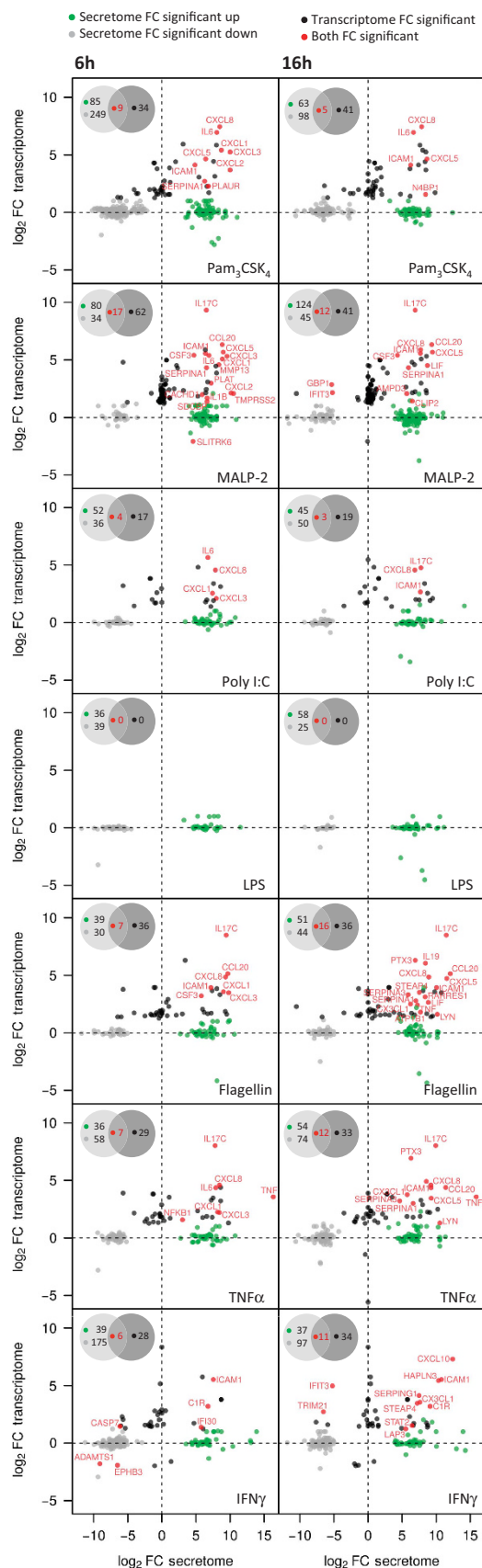


Figure 4 Correlation of receptor-induced protein secretions with transcriptional regulations. Differentially secreted proteins (x axis) and differentially expressed gene transcripts with a correspondingly secreted protein (y axis) were plotted with their respective fold changes (FC) ($P < 0.05$) for each indicated receptor stimulation. Significant FCs for both are indicated in red with their associated gene symbols. Secreted proteins that were only significantly changed on the transcriptional level are shown with black dots. The respective numbers for each fraction are shown in the respective Venn diagrams for each receptor.

(black dots, **Figure 4**). Gene expression analysis of six selected proteins that demonstrated differential secretion in response to at least two TLR agonist stimulations also showed no transcriptional regulation at 2 h, 4 h or 8 h of stimulation as depicted by qPCR (**Supplementary Figure S2b**). For the TLR2 ligands Pam₃CSK₄ and MALP-2 most correlations were found after 6 h, while for Flagellin, TNF α and IFN γ most regulated correlations were found after 16 h of stimulation (**Figure 4**). The most predominant group of transcriptionally controlled secretion of proteins were cytokines, with 15 significant correlations. We confirmed the results for six of these cytokines, i.e. CXCL5, CXCL1, IL6, LIF, CCL2, CCL20 by ELISA, verifying that the results of our MS analysis were representative and the sensitivity was in the range of 100 picogram or more (**Supplementary Figure S4b**). Several cytokines, such as CXCL8 and IL17C, were equally secreted by most receptor stimulations, indicating the induction of a comprehensive and comparable inflammatory response. The most similar cytokine secretion profiles were induced by Pam₃CSK₄, MALP-2, Flagellin, and also TNF α , which is in accordance with our transcriptome results (**Supplementary Figure S4a**). In contrast to the gene expression response, only for Flagellin 16 h after stimulation, we were able to detect a low secretion of TNF α itself, which therefore cannot explain the observed similarities (**Figure 5b**, **Supplementary Figure S4b**). Also others, such as Fractalkine, showed a more specific profile, associated with Flagellin, TNF α and IFN γ , or were found to be secreted solely in response to one receptor stimulation, such as IL19 by Flagellin (**Figures 4 and 5b** and **Supplementary Figure S4b**). These results show that the stimulation of TNFR1 provokes a very similar sensor-receptor-induced cytokine release and is therefore able to induce an equalized local inflammatory response, independent of a preceding direct pathogen exposure of each cell. The IFN γ -induced cytokine secretion profile was again different from the other receptors, with notably specific secretions of CCL2 and CXCL10.

Different biological functions for different modes of protein secretion

For further analysis of secreted proteins, we differentiated all upregulated secreted proteins on the basis of their characteristics as being transcriptionally regulated, annotated to exosomes, or independent of both but were predicted to be secreted (**Figure 5**). The remaining proteins are listed in (**Supplementary Figure S6**). We analyzed whether the proteins possess a predictable signal peptide for a classical secretion

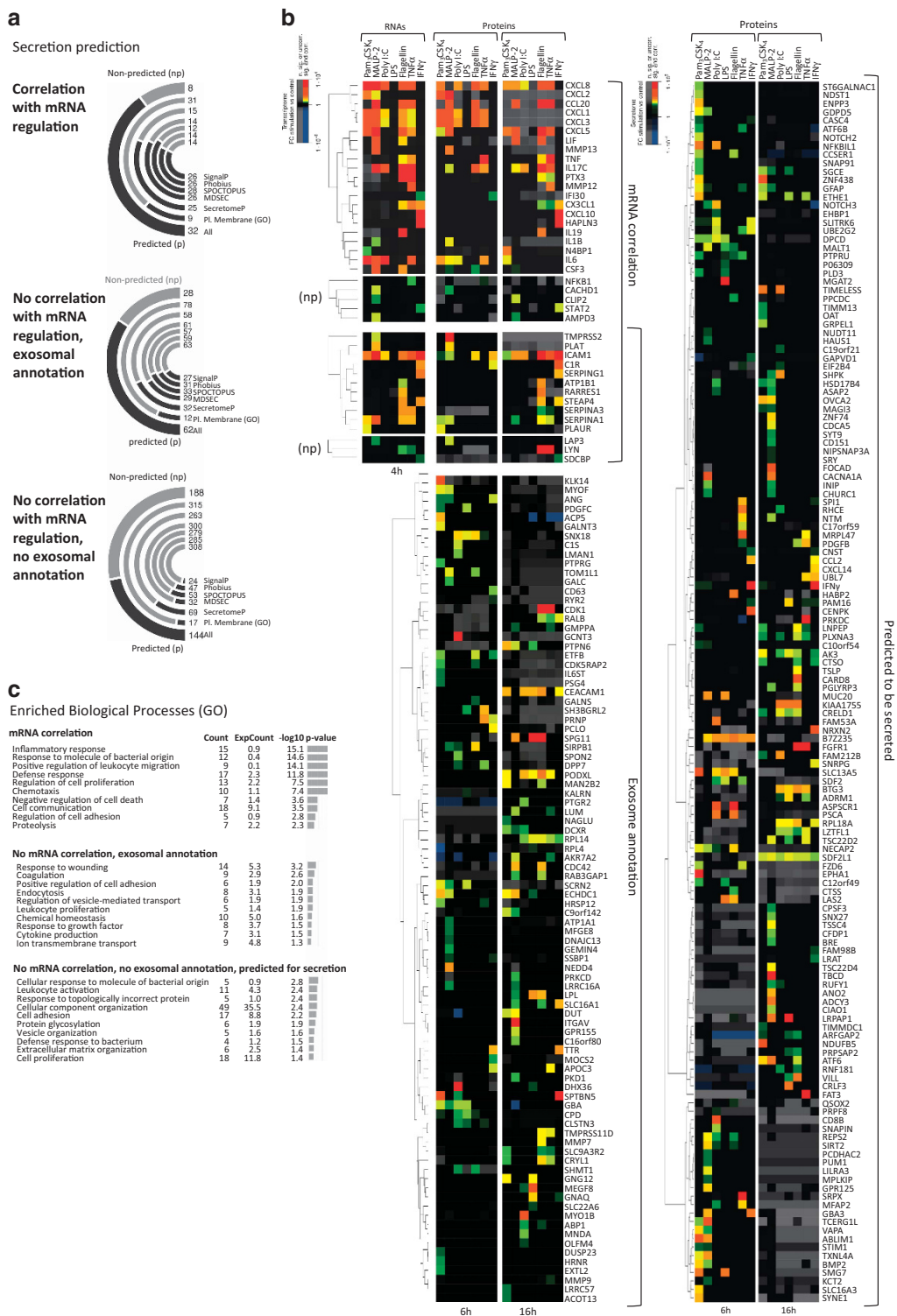


Figure 5 Characterization of receptor/ligand-induced protein secretion. **(a)** Predictions for classical and non-classical secretion mechanisms are shown in the curved bar plot. The predictions for each protein of the indicated prediction method were derived from the “Human Protein Atlas” database or a GO annotation to “plasma membrane” without concurrent annotation to “cytosol”. **(b)** The hierarchical clustering shows all secreted proteins with a correlation to mRNA expression, an annotation to exosomes or a prediction to be secreted. The clustering is based on fold changes compared to unstimulated control with a $FC \geq 2$ and a P -value < 0.05 as minimum criteria for significance. **(c)** Enrichments of “biological processes” were analyzed using GO enrichment for each indicated group. Representative categories were selected from those that were significantly enriched (P -value < 0.05 , minimum protein count of ≥ 4). Shown are the P -value for enrichment, the number of proteins accounting for each functional annotation term (Count) and the expected count in case of no enrichment (ExpCount). See also (Supplementary Table 3 online).

mechanism using the algorithms of SignalP, Phobius, SPOCTOPUS and MDSEC.^{31–34} For non-classical secretion mechanisms we used SecretomeP, and for putative shedding or exosomal membrane association the GO annotation to plasma membrane (**Figure 5a, Supplementary Figure S6**).³⁵ For most of the transcriptionally regulated proteins and also for the majority of proteins annotated to exosomes, we observed them to be very likely secreted by at least one of the secretion mechanisms considered (**Figure 5a**). For the remaining 332 proteins with no transcriptional regulation or exosomal annotation, we were able to identify 144 proteins (43.4%) with a positive prediction to be secreted (**Figures 5a and b, Supplementary Figure S6**). For proteins with a transcriptional correlation and also a positive prediction to be secreted, we observed generally higher fold changes (**Figure 5b**).

We analyzed each group for characteristic proteins and enrichments of GO annotated biological processes. Secreted proteins with a corresponding transcriptional regulation did show enrichments for inflammatory and defence responses as well as cell adhesion and migration (**Figure 5c**). Here we found 15 of all 22 secreted cytokines described in this study, confirming the transcriptionally highly regulated process of cytokine secretion. Additionally, this group contains several cytokines that were previously not associated to TLR stimulations such as IL19, LIF and CSF3. Our data verify recent results regarding IL-17C as being upregulated in response to TLR3, TLR5, and TNFR1 stimulation, in contrast to IL-17A and F that are not expressed in epithelium.³⁶ In our study, this was additionally found for the stimulation of TLR2/6 by MALP-2. Receptor ligand-specific secreted proteins were the pentraxin PTX3 (Poly I:C and TNF α , 16 h) and the two matrix metalloproteases MMP12 (TNF α , 6 and 16 h) and MMP13 (Pam₃CSK₄, 6 h). Moreover, we identified the release of the intercellular adhesion molecule ICAM1 as a transcriptionally regulated and exosome-annotated protein in response to all receptor stimulations, except for TLR4 (**Figure 5c**). Other notable transcriptionally regulated and secreted proteins were the tissue protective Alpha 1-antitrypsin (SERPINA1) for several stimulations (Pam₃CSK₄, MALP-2, Flagellin, TNF α , 6 and 16 h) and the immunomodulatory metalloredutase STEAP4 after TLR5 and IFNGR stimulation, which we also found in a previous monocytes study.³⁷ The group of exosomal annotated proteins comprised several proteins related to wound healing, such as the broad and transcriptionally independently released CEA-CAM1, a cell adhesion molecule, which has been shown to be associated with exosomes and wound healing.^{38–40} For the proteins with no transcriptional regulation we differentiated between proteins that were most likely intended to be secreted and those that more likely originated from varying forms of tissue leakage. In total, 144 proteins were identified with a positive secretion prediction (**Figures 5a,b**), while 188 proteins had no prediction for a canonical secretion mechanism (**Supplementary Figure S6**). GO analysis of the positive fraction revealed enrichments for inflammatory immune responses such as “cellular response to molecule of bacterial

origin” and “leukocyte activation”, whereas proteins with no prediction to be secreted showed enrichments for inflammation-independent processes such as “RNA processing” and “metabolic processes”. The former fraction included several disease-relevant proteins, like the bactericidal Peptidoglycan recognition protein 3 (MALP-2, Flagellin, 16 h), the chemotactic Fibroblast growth factor receptor 1 (Flagellin and TNF α , 16 h), the wound healing involved Platelet-derived growth factor subunit B (Flagellin and TNF α , 6 and 16 h) as well as the immunomodulatory cytokine Thymic stromal lymphopoietin (Flagellin, 16 h). Interestingly, the chemokines CCL2 and CXCL14 are described here for the first time as being secreted by airway ECs in response to IFN γ .

In order to confirm that LPS induced a transcriptionally independent protein secretion, we tested three of the transcriptionally unchanged proteins (PTPN6, SH3GLB2, and SDF2) by qPCR and western blot to verify their TLR4-mediated release (**Supplementary Figure S4c**).

Alarmins were not differentially secreted in response to receptor activation

Endogenous alarmins are of specific interest due to their ability to activate innate immune responses after release. We reviewed the published literature for described proteinous alarmins or DAMPs. The search revealed 48 proteinous alarmins, which are listed in (**Supplementary Table 1**). By revisiting the results of our secretome analysis, we found that 24 out of the 48 recognized alarmins were present in all supernatants of airway ECs (**Supplementary Figure S7**). However, the levels of these alarmins did not change significantly in response to any of the receptor stimulations, nor was a transcriptional activation profile observable in the untreated controls.

DISCUSSION

In this study, we performed a comprehensive transcriptome and secretome study to analyze the ligand-induced sensor responses of all expressed TLRs and the effector responses of TNFR1 and IFNGR on primary human airway ECs. Our results show that the transcription profiles induced by specific ligand stimulation of the receptor heterodimers TLR1/TLR2 (Pam₃CSK₄), TLR2/TLR6 (MALP-2), as well as TLR3 (Poly I:C) and TLR5 (Flagellin) were largely overlapping. Regulated genes were most dominantly associated with inflammatory immune responses, but in addition, several other pathways were found to be modulated. These data are in accordance with the common understanding of TLR-induced signaling pathways converging to the same central signaling nodes, such as NF- κ B, MAPK cascades and IRF circuits.⁴¹

Among all genes differentially expressed in response to TLR stimulations, a core set of 51 uniformly regulated genes was identified. This core set includes 15 cytokines upregulated in TLR-activated bronchial epithelial cells. In addition, we detected a remarkable and, until now, not described overlap of the transcriptional signatures obtained by sensor-type responses (TLR stimulation) and effector-type responses (TNFR1 stimulation), which included the regulation of 15 cytokines. In contrast to

TLR1/2, TLR2/6, TLR5 and TNFR ligation, and in accordance with other studies,^{42,43} IFNGR and TLR3 stimulation induced a divergent transcriptional expression pattern that was dominated by an anti-viral immune response. The huge overlap between TNFR and TLR signaling might be attributable to the activation of the TRAF2/p38 MAPK cascade and of NF- κ B by both receptor types.⁴⁴ In the airways, TNF α is mainly secreted by activated macrophages or by other recruited effector cells that are attracted after chemokine-release of TLR-activated epithelial cells. It can therefore be assumed, that one of the major functions of TNF α -induced signaling in the airways is to sustain and distribute the TLR-initiated inflammatory immune response in the pulmonary epithelium.

Interestingly, in the context of epithelial inflammatory immune responses, we found that LPS activation of TLR4 was not inducing any transcriptional response and consequently, no cytokine release in NHBE cells, despite detectable expression levels of TLR4 and its co-receptors CD14 and MD2. This is in accordance with other reports demonstrating a TLR4 unresponsiveness to LPS in bronchial ECs.^{11,13,45} Monick *et al.* suggested that only an additional sensitization of TLR4, e.g. by RSV infection, would lead to an epithelial cell-mediated cytokine secretion upon TLR4 ligation. LPS is usually a very potent endotoxin, and its presence in inhaled air has a high potential to induce inflammatory damage in the airway epithelium, indicating that transcriptional responses of environmental LPS-initiated TLR4 signaling in airway ECs must be tightly controlled.¹¹

Taken together, our transcriptome results demonstrate the importance of TLR, TNFR, and IFNGR signaling in airway ECs for orchestrating the transcriptional regulation of an inflammatory response.^{6,46–48} The receptor stimulation-induced protein release was found considerably less overlapping and a lot more ligand-specific in its response. Of all differentially secreted proteins the small fraction of cytokines showed the highest correlation with transcriptional regulation and was shared by TLR and TNFR ligation. Among the non-transcriptionally regulated proteins, we were able to identify a considerable number of exosome-associated secreted proteins. Diverse functional roles of these extracellular vesicles have been suggested in the lung, including homeostasis, cellular waste management, intercellular molecule exchange, and the regulation of immune responses.^{49,50} To date, only few studies have investigated the role of PRRs expressed on airway ECs for protein composition and release of exosomes.²⁹ Among the enriched annotations, we also identified wounding responses, wound healing and regulation of coagulation, suggesting an important role of epithelial cell released proteins for the restoration or maintenance of homeostasis in the airway epithelium. These biological functions were not enriched in the transcriptome analysis, suggesting that transcription-independent mechanisms are responsible for this specific EC protein secretion. A recent report about TLR4-specific protein release in the airway epithelium via exosomes supports our finding of transcription-independent protein secretion after LPS exposure. We also found a widespread but indifferent secretion of proteinous DAMPs in stimulated and unstimulated

NHBE cell culture supernatants. While this confirms an unaltered cell viability after stimulation, it also suggests that DAMP release is not regulated by TLR, TNFR1, or IFNGR stimulations.

The epithelial surface of the pulmonary mucosa consists of highly differentiated, regionally distinct epithelial cell types, each playing a specialized role in normal pulmonary function and host defense.^{51,52} In this study, we selected a model of primary human airway epithelial cells cultured in submerged monolayers in order to allow for a reduction of cell types and to decrease confounding variables in transcriptome and proteome analysis. This cellular model has often been used for studying innate immune responses to pathogens and provided important insights into the immune mechanisms.^{53,54} Though, the submerged culture of confluent bronchial ECs may recapitulate an epithelium undergoing repair, associated with slightly different responses when compared to fully differentiated cells grown in air-liquid interface cultures, it provides a simple cell culture system devoid of differentiation-evoked clara cell and goblet cell formation and avoids differences in the degree of polarization.^{26,55} In order to confirm the relevance of our data, we compared the results from our study with published data on NHBE cells grown submerged or in air-liquid interface culture. We could match 163 of 183 secreted proteins identified for non-stimulated NHBE published by the human secretome atlas in our control fraction and three more after receptor ligations.⁵⁶ With regard to apically or basolaterally secreted proteins from air liquid interface cultures of primary ECs, we found 317 out of 362 proteins (87.6%) of the apical and 221 out of 241 proteins (91.7%) of the basolateral site in cell culture supernatants in our submerged culture.⁵⁷ We therefore conclude, that the polarized differentiation of confluent NHBE cells has no strong impact on the overall secretion pattern. In comparison to protein identifications in bronchial lavages from healthy patients, we were able to confirm 182 of 251 described secreted proteins,⁵⁸ indicating that our *in vitro* model system of primary ECs represents the major protein secretion profile of the corresponding body fluids *in vivo*, though, the particular contribution of clara cells and goblet cells after TLR activation should be addressed in future studies.

A possible limitation of our study is that we measured the transcriptional response at only one time-point after 4 h of receptor stimulation. However, pilot experiments allowed us to validate the biological relevance of this time-point for NHBE stimulation, matching the kinetics of the transcriptional activation observed for other cell types.¹⁹

In conclusion, our study represents a starting point for detailed further investigations to explore the diverse receptor-induced cellular responses of airway ECs. Although very early secondary autocrine cell stimulations, as well as putative indirect stimulatory effects of the chosen receptor ligands, cannot be ruled out, our data provide a first comprehensive analysis that compares in parallel the overall responses induced by the stimulation of all expressed TLRs as well as TNFR1 and IFNGR on primary human airway ECs. The presented results of our study already indicate, that the airway epithelium exhibits a

far more complex receptor-induced cellular response, which, besides transcriptional regulations, is also based on non-transcriptionally regulated protein secretion. The diversity of the receptor-induced protein secretions seems to be greater than previously estimated.

METHODS

Cell culture. Normal human bronchial epithelial cells (NHBE) were purchased from Lonza (Cologne, Germany) and were obtained from a non-smoking healthy Caucasian female (67 years) donor. All experiments were done with NHBE cells derived from a single donor, to reduce inter-individual variances in gene transcription and protein secretion.⁵⁹ To ensure signaling functionality of all receptors activated by the corresponding ligands in these cells, the transcriptomic data set was screened for putative loss-of-function polymorphisms. Cells from this donor were used to perform stimulation experiments for the transcriptome and proteome studies as well as for the confirmatory experiments. We used submerged cell culture conditions in order to decrease variances and enable a consistent comparison between all applied stimulations in three biological replicates. Cells were seeded at a density of 8×10^4 per ml on collagen I coated tissue culture plates (BD BioCoat) and grown in BEBM basal medium supplemented with bovine pituitary extract (BPE), hydrocortisone, human epidermal growth factor (hEGF), epinephrine, transferrin, insulin, retinoic acid, triiodothyronine and gentamicin/amphotericin-b included in the NHBE-specific BEGM BulletKit (Lonza, Basel, Switzerland) as described previously.⁶⁰ Medium was changed every 2 days throughout the cell culture period. All cultures showed the characteristic cobblestone appearance of bronchial epithelial cells (**Supplementary Figure S1d**) and were used until passage 4 to 6. NHBE cells were collected when cells were covering the whole surface for 3 days. To reduce the protein complexity and abundance in the culture cell medium of NHBEs, we excluded bovine pituitary extract (BPE) supplement from the NHBE standardized culture medium during stimulation with the TLR-agonists and verified that this did not affect cell viability (**Supplementary Figure S1a-d**) or the secretion of interleukin-8 (CXCL8; **Supplementary Figure S1e**). To rule out LBP-dependency for the induction of TLR4/MD-2, signaling only rough LPS (from *Streptococcus minnesota* R595) was used in this study.⁸ Three-day confluent cells in passage number 4 were washed twice with phosphate-buffered saline (PBS) and cultured in media omitting bovine pituitary extract for given amounts of time with added indicated agonists (**Table 1**). The following receptor ligands and concentrations were used for the stimulation of NHBE cells: synthetic triacylated lipoprotein (Pam₃CSK₄, $10 \mu\text{g ml}^{-1}$, InvivoGen) for TLR1/2 (ref. 7), Macrophage-activating lipopeptide-2 (MALP-2, carrier free, 100 ng ml^{-1} , Enzo Life Sciences) for TLR2/6, low-molecular-weight polyinosine-polycytidylic acid (Poly(I:C), 100 ng ml^{-1} , InvivoGen) for TLR3, rough lipopolysaccharide (LPS) from *Streptococcus minnesota* strain R595 (100 ng ml^{-1} , InvivoGen) for TLR4, recombinant flagellin from *Salmonella typhimurium* (100 ng ml^{-1} , InvivoGen) for TLR5, tumour necrosis factor alpha (TNF α , carrier free, 100 ng ml^{-1} , R&D Systems, Minneapolis, MA) for TNFR1 and IFN γ (100 ng ml^{-1} , R&D Systems) for IFNGR. LPS was also used in conjunction with $1 \mu\text{g ml}^{-1}$ LBP (R&D systems) and $1 \mu\text{g ml}^{-1}$ sCD14 (Sigma Aldrich, Steinheim, Germany) where indicated. We were further able to show that adding soluble CD14 and LBP did not have an influence on the LPS-dependent CXCL8 cytokine release measured by ELISA (**Supplementary Figure S1e**) which was therefore not applied in later assays.

Secretome preparation. In order to consistently detect low abundant immune-modulatory proteins such as cytokines in highly complex secretomes, we applied a novel approach by combining a full secretome enrichment using low cutoff spin filters in combination with a direct

phase transfer based in-solution digestion to minimize protein loss and sample to sample bias.^{61,62} 10 ml medium from confluent grown NHBE cells were collected and spun down at 200 g for 5 min. The supernatant was collected and spun down again at 4500 g for 10 min. For later RNA sequencing analysis, the remaining confluent grown cells were released using 0.25 % Trypsin-0.1 % EDTA and pelleted by centrifugation at 200 g for 5 min. The pellet was lysed in 600 μl RLT buffer (Qiagen) and stored in a frozen state for later use. The supernatant was concentrated to a final volume of 50 μl using 3 kD MWCO centrifugal filtration units (Amicon Ultra, EMD Millipore, Schwalbach, Germany). An equal amount of sample corresponding to 10 μg protein was diluted into a final volume of 50 μl digestion buffer (50 mM ammonium bicarbonate, 0.5% sodium deoxycholate (SDC), 10 mM DTT and digested by addition of the protease trypsin in a 1:50 ratio for 16 h at 37 °C. The digested sample was acidified by the addition of 0.5% formic acid to precipitate SDC. Ten volumes of ethyl acetate were added to the sample and vortexed to remove SDC by phase transfer. The settled, non-aqueous upper phase was removed and the procedure repeated twice. The remaining aqueous peptide phase was dried using a vacuum centrifuge (SpeedVac, Thermo Fisher) and the peptides reconstituted into 20 μl of 0.1% formic acid and 2% acetonitrile in water.

Glycoproteome preparation. A total of 1×10^7 cells were extensively washed with PBS and scraped into 100 μl of 2% SDS/PBS. After heating at 95 °C for 5 min., samples were stored at -20 °C until further use. After thawing, lysates were centrifuged at 20,000 g for 20 min. The supernatant was subjected to buffer exchange using polyacrylamide spin desalting columns (7K MWCO, Thermo Fisher) equilibrated with 100 mM sodium acetate, pH 5.5. Samples were oxidized with 10 mM sodium periodate for 30 min. at room temperature in the dark. The sodium periodate was removed by a second buffer exchange using polyacrylamide desalting spin columns equilibrated with PBS pH 7.5. Oxidized sugar groups were immobilized on 50 μl (bead volume) Ultralink Hydrazide Gel (Thermo Fisher) overnight at room temperature. Non-glycoproteins were removed by washing the resin three times with 1% SDS/PBS, 8M Urea in 100 mM Tris/HCl pH 8.0, 1M NaCl in 100 mM Tris/HCl pH 8.0, 20% CH₃CN / 10 mM Tris/HCl pH 8.0. After the second urea wash, glycoproteins were reduced by the addition of 100 mM DTT in 8 M Urea Tris/HCl pH 8.0 (60 min, room temperature). After a brief wash, cysteins were alkylated with 50 mM iodoacetamide in 8 M Urea 100 mM Tris/HCl pH 8.0 (30 min, room temperature in the dark). After washing, the resin was equilibrated with 50 mM NH₄HCO₃ and re-suspended in 30 μl 50 mM NH₄HCO₃ containing trypsin in a ratio of 1:100 (sequencing grade, Thermo Fisher) and digested on resin overnight at 37 °C. The next day, trypsin-released peptides (GlycoProt fraction) were collected and dried in a centrifugal evaporator (SpeedVac, Thermo Scientific). The resin was again extensively washed (procedure as in the beginning) and re-suspended in 50 mM NH₄HCO₃ containing 0.5 U PNGaseF per sample. After enzymatic release of N-glycopeptides (37 °C, overnight), the deglycosylated peptides (GlycoPep fraction) released were collected and dried in a centrifugal evaporator (SpeedVac, Thermo Scientific, Idstein, Germany).

Secretome analysis by mass spectrometry. Each digested peptide sample of each biological replicate was analyzed three times by an UHPLC (RSLC, Thermo Scientific) coupled Orbitrap Velos Pro LC-MS/MS system (Thermo Scientific). Two micrograms of peptides were applied onto a C18 reverse-phase PepMap 50 cm fused silica capillary column (75 μm ID) and separated using a 300 min, non-linear gradient from 3 to 95% acetonitrile/0.1% formic acid at 300 nL min⁻¹. Eluting peptides were analyzed using automated data-dependent acquisition in which each MS scan (250–1600 m/z) was acquired at a resolution of 60 000 FWHM and followed by a maximum of 20 MS/MS scans at a resolution of 7,500 FWHM using HCD (normalized collision energy of 30). The maximum allowed ion injection time was set to 500 ms for MS and MS/MS scans. The automatic gain control (AGC) target values

Table 1 Sequence of forward and reverse primers of indicated target genes and the size of each PCR product.

Human gene	Symbol	Forward primer	Reverse primer	Size (bp)
C-C motif chemokine 20	CCL20	5-GTCTGTGTGCGCAAATCCAA-3	5-GCAAGTGAACCTCCAACCC-3	159
CD63 antigen	CD63	5-TCCATGTGGAAGAACCGAGTC-3	5-TCCACACAGCCCTCCTTATG-3	104
CD9 antigen	CD9	5-TCCACTATGCGTTGAAGTCTG-3	5-ATGGCATCAGGACAGGACTT-3	118
CEACAM1	CEACAM1	5-CAGGACCACAGTCAAGACGA-3	5-GGTTGCTGGGCTTCAAAGTT-3	167
C-X-C motif chemokine 1	CXCL1	5-CTCAATCCTGCATCCCCCAT-3	5-TTCCTCCTCCCTTCTGGTCA-3	86
C-X-C motif chemokine 2	CXCL2	5-GAAAGCTTGTCTCAACCCCG-3	5-CACATTAGGCGCAATCCAGG-3	196
Cyclin-dependent kinase 1	CDK1	5-AGTCAGTCTTCAGGATGTGCTT-3	5-CCATGTACTGACCAGGAGGGAT-3	113
Endophilin-B2	SH3GLB2	5-GTTTGACCGGCAAGCAGAAG-3	5-AGCACTGTGCGTAGTAGGTT-3	122
Ethylmalonyl-CoA decarboxylase	ECHDC1	5-ATAAGTGTGCGCTGGTTCA-3	5-ACTCTCTGGAGTCATTAACTGA-3	90
Hypoxanthine-guanine phosphoribosyltransferase	HPRT1	5-GACCAGTCAACAGGGGACAT-3	5-AACACTTCGTGGGGTCTTTTC-3	195
Interferon gamma receptor 1	IFNGR1	5-GAGACGAGCAGGAAGTCGAT-3	5-TGGCACTGAATCTCGTCACA-3	142
Interferon gamma receptor 2	IFNGR2	5-CCTCTCCCTTTGACATCGCT-3	5-TTCCAAAGCAGTTGTGCCTG-3	178
Interleukin 17c	IL17C	5-CCTGGAGATACCGTGTGGAC-3	5-GTGCATCGATACAGCCTCTG-3	90
Interleukin 6	IL6	5-GAGGAGACTTGCTGGTGAA-3	5-TGGGTCAGGGGTGGTTATTG-3	186
Interleukin 8	CXCL8	5-TCCAAACCTTTCCACCCCAA-3	5-ACTTCTCCACAACCTCTGC-3	154
Peptidyl-prolyl cis-trans isomerase B	PPIB	5-ATGTAGGCCGGGTGATCTTT-3	5-TGAAGTTCTCATCGGGGAAG-3	219
Protein BTG3	BTG3	5-AGGCAGTTGAGAGGTTTGCT-3	5-ACGAATACATCTGTAGGCCTGT-3	110
Spatacsin	SPG11	5-CCTCACTGGCATTGGAAGGT-3	5-TTTCAGGGTACCACTCGGAT-3	115
Stromal cell-derived factor 2	SDF2	5-GGCTCCGCGATACAGTTAGG-3	5-CCCACTACCTGACCCATAGC-3	179
Toll-like receptor 1	TLR1	5-CAGGCCCTCTTCTCGTTAG-3	5-TGGCAAAATGGAAGATGCTAGT-3	157
Toll-like receptor 2	TLR2	5-TGCATTCCCAAGACACTGGA-3	5-AGGGAGGCATCTGGTAGAGT-3	131
Toll-like receptor 3	TLR3	5-GCCTTCTGCACGAATTTGACT-3	5-CCAGCTGAACCTGAGTTCTTA-3	154
Toll-like receptor 4	TLR4	5-CAACCTCCCTTCTCAACCA-3	5-CTGGATGGGGTTTCTGTCA-3	196
Toll-like receptor 5	TLR5	5-GCTACTGACAACGTGGCTTC-3	5-ACATCTGAGGCTCCGACATC-3	176
Toll-like receptor 6	TLR6	5-GCCCTGGTATCTCAGGATGG-3	5-TCACTTTTACCCAGGCAGA-3	144
Toll-like receptor 7	TLR7	5-ATCTTGGCACCTCTCATGCT-3	5-ACCATCTAGCCCCAAGGAGT-3	158
Toll-like receptor 8	TLR8	5-GTTTCTCTTCTCGGCCACCT-3	5-GGCGCATAACTCACAGGAAC-3	164
Toll-like receptor 9	TLR9	5-GAAGGGACCTCGAGTGTGAA-3	5-CTCACAGGGTAGGAAGGCAG-3	196
Tumor necrosis factor receptor 1	TNFRSF1A	5-TGTGCCTACCCAGATTGAG-3	5-CCTTCAAGCTCCCCCTCTTT-3	202
Tumor necrosis factor receptor 2	TNFRSF1B	5-GAGGACAGCACATACACCA-3	5-GAGTGCAGGCTTGAGTTCC-3	100
Tyrosine-protein phosphatase non-receptor type 6	PTPN6	5-TCTCGCTCTCCGTCAGGG T-3	5-TTCAGCGGGTACTTGAGGTG-3	187
Zinc finger FYVE domain-containing protein 26	ZFYVE26	5-CCTCAGAGGGAGAAACGATCAG-3	5-CTGGAGATACCAGGAGGAGCA-3	131

were set to 1×10^6 counts for MS and 5×10^4 for MS/MS scans. A dynamic MS2 mass exclusion time window of 60 s was set including a maximum of 500 proteins in a 10 ppm maximum delta mass window.

Glycoproteome analysis using mass spectrometry. Tryptic and deglycosylated peptides were analyzed with an UHPLC (RSLC, Thermo Scientific) coupled Orbitrap Fusion LC-MS/MS system (Thermo Scientific) in triplicate runs. Full MS scans were acquired with a resolution of 120,000 FWHM in the Orbitrap analyser (m/z range 400–1,600, quadrupole isolation) during a 140 min, non-linear gradient from 2 to 95% acetonitrile / 0.1% formic acid. MS1 precursors were fragmented by higher energy collisional dissociation (HCD, 30% collision energy) and fragment ion spectra were acquired in the order

highest to least charge and least to highest intensity during a 4 second maximum cycle time in the ion trap in rapid mode. The following conditions were used: spray voltage of 2.0 kV, heated capillary temperature of 275 °C, S-lens RF level of 60%, maximum AGC value of 5×10^5 counts for MS1 with a maximum ion accumulation time of 50 ms and a maximum AGC value of 5×10^4 counts for MS2 with a maximum ion accumulation time of 35 ms. A dynamic MS2 mass exclusion time window of 30 s was set with a 10 ppm maximum mass window.

Protein identification and quantification. Secretome raw data was processed utilising Proteome Discoverer v1.4.0.280 software (Thermo Scientific) using a target FDR of 0.01 on peptide level and default parameters if not indicated otherwise. The human UniProt database

(version 05.2013) was searched using Sequest HT and Mascot (version 2.4, Matrix Science) with 10 ppm peptide and 0.05 Da fragment ion tolerances. Trypsin, with the possibility of two missed cleavages, was selected as enzyme. The following variable modifications were allowed: oxidation (H/M/W), phosphorylation (S/T/Y), acetylation (K) and methylation (K/R). The Percolator v2.1 node was used for peptide validation based on *q*-value. Each technical triplicate from a biological triplicate sample was calculated in a MudPIT scheme. Glycoproteomic raw data was processed utilising Proteome Discoverer v2.1.0.81 software with Sequest HT search engine using a target FDR of 0.01 on peptide level and default parameters if not indicated otherwise. The human UniProt database (version 05.2013) was searched using Sequest HT with 10 p.p.m. peptide and 0.5 Da fragment ion tolerances. Trypsin, with the possibility of two missed cleavages, was selected as enzyme. The following modifications were allowed: oxidation (M) and deamidation (N/Q) as variable, carbamidomethylation (C) as fixed modification. The integrated Percolator node was used for peptide validation based on *q*-value. Proteins were quantified by Proteome Discoverer based on the calculation of the area under the curve (AUC) from the three highest extracted peptide ion chromatograms (XICs) of each protein (Top3 method).⁶³ All resulting data were imported as a single multi-consensus report into Proteome Discoverer and exported as CSV data for further analysis in R. Unless otherwise stated, all follow-up data analysis was carried out using R version 3.1.1 and R packages (R Core Team 2014). For peptide to protein inference, abundances of peptides that were only quantified in one sample and were the only peptides quantified in that particular sample for a particular protein group were set to zero. Protein abundances for each sample were calculated as mean of the three highest abundances for all remaining peptide abundances for each sample and each protein group. To reduce effects of false negatives due to inherent under-sampling by mass spectrometry, we implemented additional stringency by testing significance against two additional control samples (all in triplicates). Due to the limited sensitivity of mass spectrometry and algorithms used in peptide identification, data-dependent analysis produces zero entries if peptides fall below a varying detection limit. In our study, rather than imputing missing values, a strategy was chosen that included the measurements of all other replicates of a particular stimulation as well. Zeros were considered false negative if at least one of the other replicates showed a protein abundance different from zero. These zeros were set to “not assigned” (NA) for further analysis. If, on the other hand, all replicates of a particular stimulation were zero, one abundance was set to the detection limit after normalization and all others were set to NA. Overall, this strategy avoids sample replicates that show artificially low or high variances by reducing or even deleting information about sample variance and, therefore, with respect to statistical testing, relies on a linear modelling approach that borrows information from other samples. Remaining zeros and NAs were not included in the subsequent normalization step. Log2 transformed data was normalized using the “normalizeBetweenArrays” function of the R package “limma” version 3.20.7 with method “quantile”. After normalization, all remaining original zeros were set to the lowest value of the normalized data set. A linear model was used to assess differential protein secretion. The model was set up using “limma” and fitted to the contrasts between all stimulations and the unstimulated controls for each time point. Moderated *t*-statistics were calculated using functions “treat” and “topTreat” of “limma”. *P*-values were adjusted according to the method of Benjamini and Hochberg. Adjusted *P*-values below 0.05 were considered significant. Tests were performed against the null hypothesis that the absolute value of log2 fold change is smaller or equal to one. Additional filters were applied to avoid false positive or negative significant protein contrasts. First, significant contrasts only induced by filtering out of solitary peptides in the peptide to protein inference step were not considered significant. Second, some proteins are difficult to detect by tandem MS and abundances are quantified only occasionally by chance. To avoid false positives and negatives due to this effect, only contrasts that were based

on proteins which were at least quantified in two biological replicates for at least one biological sample were considered significant.

mRNA preparation. Equal amounts of RLT buffer lysed NHBE cells ($\sim 5 \times 10^6$ cells) were further processed using the RNeasy RNA isolation kit following the manufacturer's instructions (Qiagen). cDNA libraries were generated and sequenced in paired-end mode (2×100 bp) on a HighSeq 2000 by Eurofins Genomics, Ebersberg, Germany. The raw files were processed by Eurofins by applying RTA 1.17.21.3 and bcl2fastq-1.8.4 to generate the fastq-files of all sequenced short reads for each of the 33 samples. All results were obtained from biological triplicates with a mean sequencing depth of 21.7 million reads per sample. The raw sequence data were stored in the Sequence Read Archive at the National Center for Biotechnology Information (NCBI) under accession number: SRP057579.

Exosome quantification. Supernatants were collected after 16 h of stimulation and centrifuged at 400 g for 20 min to remove cells and larger cell debris. The cleared supernatant was sequentially centrifuged at 16 000 g for 20 min to remove any remaining cell debris. The amounts of exosomes were quantified by ELISA using the ExoQuant Overall Exosome Capture and Quantification Assay Kit (BioVision) according to the manufacturer's instructions.

RNA sequencing data analysis. Sequence quality of each fastq-file was assessed using fastqc (version 0.11.1). All remaining TruSeq adapters were trimmed using cutadapt (version 1.4). The trimmed short reads for each sample were aligned onto the human genome (hg19) by applying the STAR 2.3.0 aligner using default parameter settings. Subsequently, the resulting sam-files were converted to bam-files using SAMtools view -bS (version 0.1.19) and the total counts of short reads for each gene of hg19 for each sample, were obtained by applying featureCounts, which is part of subread-1.4.5. To allocate the gene information needed by featureCounts, the hg19-gtf-file was downloaded from Illumina iGenomes (UCSC archive: 2014-06-02-13-47-56). The tables of total counts of short reads for each sample were imported into R (version 3.1.1). DESeq2 (DESeq2 release 1.6.3, Bioconductor version 2.14)⁶⁴ was used to analyze the differential gene expression of the treated samples vs. the untreated samples, referred to as control, with the contrast-option as well as cooks Cutoff-filtering set FALSE, independent filtering set TRUE, log2FoldChange (log2FC) threshold set to 1, and an adjusted *P*-value cutoff of 0.05. Additionally, all treatment-specific samples were analyzed with regard to their differential expression vs. all other treated samples applying DESeq2 again with the same parameter settings as mentioned above. Then, by intersection of all differentially expressed genes (DEGs) per sample vs. their control and vs. all other treated samples, the DEGs that were specifically up- and downregulated in only one treatment-specific setting were identified for each treatment.

Identification and comparison of specific responses. Genes or proteins were considered specific for a particular stimulation or combination of stimulations, when tests against controls, as well as against all other remaining stimulations, were significant. A transcript and its corresponding protein product were considered to show a correlation between the transcriptional and the secretory response when at least for one stimulation the transcriptome and the secretome at any of the two time points showed a significant fold change in the same direction.

Gene ontology classification. Version 3.0.0 of the R package “org.Hs.eg.db” was used for all GO classifications (version 24.09.2014). The human proteome as defined by the UniProt database (version 05.2013) was used as reference for annotation enrichments.

Visualization of results. Heat maps were hierarchically clustered in one or two dimensions, as appropriate, using Ward's minimum variance method implemented in the R function “hclust” with method “ward.D2”.⁶⁵ All fold changes—significant and non-significant—were

used for clustering. Significant fold changes are shown in colour and non-significant fold changes in different shades of grey. Error bars of bar plots show s.d.

Pathway enrichment. Enriched pathways were identified with KOBAS 2.0 (KEGG Orthology Based Annotation System) software using all significantly up- and downregulated genes compared to control. The genes were annotated including pathways from the databases PID, BioCarta (from PID), Reactome and PANTHER (Protein Analysis THrough Evolutionary Relationships). The statistical enrichment significance was tested using Fisher's exact test (one-sided) and visualized by R. The human UniProt protein database was used as background (version July 2014) and the final list filtered against annotated diseases.

Cytokine concentration determination by ELISA. Cytokine assays were performed using ProcartaPlex multiplex immunoassays (eBioscience) according to the manufacturer's instructions. Briefly, NHBE cells were incubated with the respective agonists in media omitting bovine pituitary extract for 16h. The collected supernatants were incubated with magnetic antibody beads in duplicates in a ninety-six-well plate overnight at 4 °C. Next, 25 µl of detection antibody were added to each well and incubated for 30 min. Streptavidin/Phycoerythrin solution was added to each well (50 µl per well) and incubated for a further 30 min incubation period. All mandatory washing steps were repeated three times. After addition of 120 µl reading buffer, the plate was read by a Bio-Plex 200 analyser (Bio-Rad, Hercules, CA, USA). The cytokine concentrations were extrapolated from standard curves using Bio-Plex 5.0 software (Bio-Rad). IL-8 cytokine secretion was also quantified using a human IL-8 ELISA detection set (BD Biosciences, Heidelberg, Germany) according to the manufacturer's protocols. Measurements were made as triplicates in a microplate reader (Tecan).

Gene expression analysis by qPCR. Complementary DNA (cDNA) was synthesized from 2 µg of RNA using the High Capacity cDNA Reverse Transcription Kit (Applied Biosystems, Foster City, CA) and following manufacturer's instructions. For PCR analysis, specific primers for each target gene were designed using the online primer-BLAST tool of the National Center for Biotechnology Information (NCBI, <http://www.ncbi.nlm.nih.gov/tools/primer-blast>). The sequences of all primers used for amplification are listed in **Table 1**. PCR of the cDNA was performed on a S1000 Thermal Cycler (Bio-Rad, Watford, UK) in a 25 µl reaction volume containing 0.2 µM primers, 1 U Taq DNA polymerase (5-Prime, Hamburg, Germany) and 200 µM dNTPs. Thermal conditions included an initial 95 °C denaturation step for 3 min and then 35 cycles of 10 s at 94 °C, 30 s at 60 °C and 30 s at 72 °C. The resulting PCR products were separated by gel electrophoresis, stained with ethidium bromide and visualized under a UV - trans-illuminator. Quantification of the relative expression of each target gene was carried out by qPCR on a Corbett Rotor-Gene 6000 (Qiagen, Hilden, Germany). Each sample was analyzed in duplicate in a total reaction volume of 20 µl containing 10 µl of 2 × SensiMix SYBR Master Mix (Bioline, London, UK) and 0.2 µM of each primer. Reactions were set up using a CAS-1200 pipetting robot (Qiagen, Germany). The cycling conditions were 95 °C for 10 min followed by 40 cycles of 95 °C for 15 s, 60 °C for 20 s and 72 °C for 20 s. An RT-negative sample was included as control. Specificity of the qPCRs was assessed by melting curve analysis and size verification by electrophoresis. The relative expression of the target genes was calculated using the Pfaffl method,⁶⁶ normalized to the expression of the two housekeeping genes HPRT1 and PPIB.

Western blot. Supernatants from secretome preparations were boiled for 5 min. in SDS-PAGE load buffer (1% LDS, 10% glycerol, 10 mM Tris/HCl pH 7.6, 1 mM, DTT, 0.01% Coomassie G250). 5 µg of each sample was separated on 8–16% SDS-PAGE gels (Precise, Thermo Scientific). Following electrophoresis, gels were blotted onto

nitrocellulose membranes (Millipore) and blocked with blocking buffer (5% dried milk powder in TBS) for 1 h. The blots were incubated with anti-PTPN6 (HPA001466, Sigma Aldrich), anti-SH3GLB2 (SAB1400646, Sigma Aldrich), anti-SDF2 (AV48718, Sigma Aldrich), anti-pan 14-3-3 (sc-1657, Santa Cruz) or anti-MD-2 (SAB1410439, Sigma Aldrich) diluted 1:500 in blocking buffer overnight. After washing with TBS-T (0.05 % Tween-20 in TBS), the membranes were incubated for 1 h with respective peroxidase-conjugated secondary antibodies. The blots were washed four times in TBS-T between antibody incubations and all antibodies were diluted in TBS-T containing 5% skimmed milk. Membranes were developed using ECL (Thermo Scientific).

Flow cytometry. Single cell suspensions of NHBE cells were fixed for 10 min. with a solution of 4% formaldehyde in PBS. Cells were blocked for 30 min. in 1% BSA in PBS and then stained using anti-E-cadherin (NBP2-16258, Novus Biologicals, Cambridge, UK), anti-CC10 antibody (T-18, Santa Cruz Biotechnology, Heidelberg, Germany) and anti-Vimentin (550513, BD). After 3 washing steps using 1% FCS in PBS, the cells were stained using respective APC (Santa Cruz Biotechnology) and PE (eBioscience, Frankfurt, Germany) conjugated antibodies. Controls were stained using secondary antibodies alone. For cell viability analyses, single-cell suspensions of NHBE cells were prepared and incubated as described by the manufacturer's instructions using an Annexin V-FITC apoptosis detection Kit (eBioscience). Stained cells were analyzed on a FACS Aria 2 instrument (BD Biosciences) using FACSDiva software (BD Biosciences).

LDH cytotoxicity assay. Activity of LDH in the medium was determined using a commercially available kit from Roche. Aliquots of supernatant media and reagent were mixed in a ninety-six-well plate and absorbance was recorded using a microplate spectrophotometer system (Infinite 200 Pro, Tecan, Männedorf, Switzerland). Results were analyzed using supplied Magellan software (version 6.6 Tecan).

SUPPLEMENTARY MATERIAL is linked to the online version of the paper at <http://www.nature.com/mi>

ACKNOWLEDGMENTS

We thank Andreas Otto and Dörte Becher for scientific discussions regarding mass spectrometry and method development. This study was supported by the Federal Ministry of Education and Research (BMBF), Germany, FZK 03Z2JN22 and by the DFG within the framework of the Collaborative Research Center/Transregio 124 "Pathogenic fungi and their human host: Networks of Interaction"—Project A5, both to H.S. Reviewer account details are as follows: Username: reviewer57220@ebi.ac.uk. Password: kUUzuZOB. The RNA sequencing data have been deposited at the NCBI in the Sequence Read Archive (SRA) under accession number SRP057579.

Accession codes: Proteomics data have been deposited at the ProteomeXchange Consortium (<http://proteomecentral.proteomexchange.org>) via the PRIDE partner repository (data set identifier PXD003548).

AUTHOR CONTRIBUTIONS

H.S. and R.L. conceived the project and designed the research; R.L. performed the experiments for secretome characterization and mass spectrometry analysis; R.L., T.E.K., and M.S. performed the experiments for transcriptome characterization; M.M.M. carried out the glycoproteome analysis; C.M. and A.H. did the qPCR experiments; R.L., D.D., T.E.K., M.S., T.C., UK.S., R.G., and H.S. performed the analysis and interpretation of results from transcriptome and secretome data; R.L., D.D., and H.S. prepared the figures, R.L. and H.S. wrote the manuscript and H.S. supervised the study. All authors discussed the results and commented on the manuscript.

DISCLOSURE

The authors declared no conflict of interest.

REFERENCES

1. Mitchell, P.D. & O'Byrne, P.M. Epithelial derived cytokines in asthma. *Chest* **151**, 1338–1344 (2017).
2. Gohy, S.T., Hupin, C., Pilette, C. & Ladjemi, M.Z. Chronic inflammatory airway diseases: the central role of the epithelium revisited. *Clin. Exp. Allergy* **46**, 529–542 (2016).
3. Schiller, H.B., Fernandez, I.E., Burgstaller, G., Schaab, C., Scheltema, R.A. & Schwarzmayr, T. *et al.* Time- and compartment-resolved proteome profiling of the extracellular niche in lung injury and repair. *Mol. Syst. Biol.* **11**, 819 (2015).
4. Peters-Hall, J.R., Brown, K.J., Pillai, D.K., Tomney, A., Garvin, L.M. & Wu, X. *et al.* Quantitative proteomics reveals an altered cystic fibrosis in vitro bronchial epithelial secretome. *Am. J. Respir. Cell Mol. Biol.* **53**, 22–32 (2015).
5. Takeda, K. & Akira, S. Toll-like receptors. *Curr. Protoc. Immunol.* **109**, 14.12.11–14.12.10 (2015).
6. Whitsett, J.A. & Alenghat, T. Respiratory epithelial cells orchestrate pulmonary innate immunity. *Nat. Immunol.* **16**, 27–35 (2014).
7. Ozinsky, A., Underhill, D.M., Fontenot, J.D., Hajjar, A.M., Smith, K.D. & Wilson, C.B. *et al.* The repertoire for pattern recognition of pathogens by the innate immune system is defined by cooperation between toll-like receptors. *Proc. Natl Acad. Sci. USA* **97**, 13766–13771 (2000).
8. Huber, M., Kalis, C., Keck, S., Jiang, Z., Georgel, P. & Du, X. *et al.* R-form LPS, the master key to the activation of TLR4/MD-2-positive cells. *Eur. J. Immunol.* **36**, 701–711 (2006).
9. Botos, I., Segal, D.M. & Davies, D.R. The structural biology of Toll-like receptors. *Structure* **19**, 447–459 (2011).
10. Guillot, L., Medjane, S., Le-Barillec, K., Balloy, V., Danel, C. & Chignard, M. *et al.* Response of human pulmonary epithelial cells to lipopolysaccharide involves Toll-like receptor 4 (TLR4)-dependent signaling pathways: evidence for an intracellular compartmentalization of TLR4. *J. Biol. Chem.* **279**, 2712–2718 (2004).
11. Muir, A., Soong, G., Sokol, S., Reddy, B., Gomez, M.I. & Van Heeckeren, A. *et al.* Toll-like receptors in normal and cystic fibrosis airway epithelial cells. *Am. J. Respir. Cell Mol. Biol.* **30**, 777–783 (2004).
12. Mayer, A.K., Muehmer, M., Mages, J., Gueinzus, K., Hess, C. & Heeg, K. *et al.* Differential recognition of TLR-dependent microbial ligands in human bronchial epithelial cells. *J. Immunol.* **178**, 3134–3142 (2007).
13. Monick, M.M., Yarovsky, T.O., Powers, L.S., Butler, N.S., Carter, A.B. & Gudmundsson, G. *et al.* Respiratory syncytial virus up-regulates TLR4 and sensitizes airway epithelial cells to endotoxin. *J. Biol. Chem.* **278**, 53035–53044 (2003).
14. Schulz, C., Farkas, L., Wolf, K., Kratzel, K., Eissner, G. & Pfeifer, M. Differences in LPS-induced activation of bronchial epithelial cells (BEAS-2B) and type II-like pneumocytes (A-549). *Scand. J. Immunol.* **56**, 294–302 (2002).
15. Mizgerd, J.P. Acute lower respiratory tract infection. *N. Engl. J. Med.* **358**, 716–727 (2008).
16. Alsina, L., Israelsson, E., Altman, M.C., Dang, K.K., Ghandil, P. & Israel, L. *et al.* A narrow repertoire of transcriptional modules responsive to pyogenic bacteria is impaired in patients carrying loss-of-function mutations in MYD88 or IRAK4. *Nat. Immunol.* **15**, 1134–1142 (2014).
17. Shaykhi, R., Behr, J. & Bals, R. Microbial patterns signaling via Toll-like receptors 2 and 5 contribute to epithelial repair, growth and survival. *PLoS ONE* **3**, e1393 (2008).
18. Parker, D. & Prince, A. Innate immunity in the respiratory epithelium. *Am. J. Respir. Cell Mol. Biol.* **45**, 189–201 (2011).
19. Meissner, F., Scheltema, R.A., Mollenkopf, H.J. & Mann, M. Direct proteomic quantification of the secretome of activated immune cells. *Science* **340**, 475–478 (2013).
20. Iwasaki, A. & Medzhitov, R. Control of adaptive immunity by the innate immune system. *Nat. Immunol.* **16**, 343–353 (2015).
21. Mukhopadhyay, S., Hoidal, J.R. & Mukherjee, T.K. Role of TNF α in pulmonary pathophysiology. *Respir. Res.* **7**, 125 (2006).
22. Desvignes, L. & Ernst, J.D. Interferon-gamma-responsive nonhematopoietic cells regulate the immune response to Mycobacterium tuberculosis. *Immunity* **31**, 974–985 (2009).
23. Hammad, H. & Lambrecht, B.N. Barrier epithelial cells and the control of type 2 immunity. *Immunity* **43**, 29–40 (2015).
24. Hackett, B.P. & Gitlin, J.D. Cell-specific expression of a Clara cell secretory protein-human growth hormone gene in the bronchiolar epithelium of transgenic mice. *Proc. Natl Acad. Sci. USA* **89**, 9079–9083 (1992).
25. Kawai, T. & Akira, S. Toll-like receptors and their crosstalk with other innate receptors in infection and immunity. *Immunity* **34**, 637–650 (2011).
26. Clark, J.G., Kim, K.H., Basom, R.S. & Gharib, S.A. Plasticity of airway epithelial cell transcriptome in response to flagellin. *PLoS ONE* **10**, e0115486 (2015).
27. Gottschalk, R.A., Martins, A.J., Angermann, B.R., Dutta, B., Ng, C.E. & Uderhardt, S. *et al.* Distinct NF- κ B and MAPK activation thresholds uncouple steady-state microbe sensing from anti-pathogen inflammatory responses. *Cell Syst.* **2**, 378–390 (2016).
28. Yang, J., Hooper, W.C., Phillips, D.J., Tondella, M.L. & Talkington, D.F. Induction of proinflammatory cytokines in human lung epithelial cells during Chlamydia pneumoniae infection. *Infect Immun.* **71**, 614–620 (2003).
29. Kesimer, M., Scull, M., Brighton, B., DeMaria, G., Burns, K. & O'Neal, W. *et al.* Characterization of exosome-like vesicles released from human tracheobronchial ciliated epithelium: a possible role in innate defense. *FASEB J.* **23**, 1858–1868 (2009).
30. Keerthikumar, S., Chisanga, D., Ariyaratne, D., Al Saffar, H., Anand, S. & Zhao, K. *et al.* ExoCarta: a web-based compendium of exosomal cargo. *J. Mol. Biol.* **428**, 688–692 (2016).
31. Kall, L., Krogh, A. & Sonnhammer, E.L. A combined transmembrane topology and signal peptide prediction method. *J. Mol. Biol.* **338**, 1027–1036 (2004).
32. Viklund, H., Bernsel, A., Skwark, M. & Elofsson, A. SPOCTOPUS: a combined predictor of signal peptides and membrane protein topology. *Bioinformatics* **24**, 2928–2929 (2008).
33. Petersen, T.N., Brunak, S., von Heijne, G. & Nielsen, H. SignalP 4.0: discriminating signal peptides from transmembrane regions. *Nat. Methods* **8**, 785–786 (2011).
34. Uhlen, M., Oksvold, P., Fagerberg, L., Lundberg, E., Jonasson, K. & Forsberg, M. *et al.* Towards a knowledge-based Human Protein Atlas. *Nat. Biotechnol.* **28**, 1248–1250 (2010).
35. Garton, K.J., Gough, P.J. & Raines, E.W. Emerging roles for ectodomain shedding in the regulation of inflammatory responses. *J. Leukoc. Biol.* **79**, 1105–1116 (2006).
36. Ramirez-Carrozzi, V., Sambandam, A., Luis, E., Lin, Z., Jeet, S. & Lesch, J. *et al.* IL-17C regulates the innate immune function of epithelial cells in an autocrine manner. *Nat. Immunol.* **12**, 1159–1166 (2011).
37. Muller, M.M., Lehmann, R., Klassert, T.E., Reifensstein, S., Conrad, T. & Moore, C. *et al.* Global analysis of glycoproteins identifies markers of endotoxin tolerant monocytes and GPR84 as a modulator of TNF α expression. *Sci. Rep.* **7**, 838 (2017).
38. Muturi, H.T., Dreesen, J.D., Niewski, E., Jastrow, H., Giebel, B. & Ergun, S. *et al.* Tumor and endothelial cell-derived microvesicles carry distinct CEACAMs and influence T-cell behavior. *PLoS ONE* **8**, e74654 (2013).
39. LeBlanc, S., Arabzadeh, A., Benlolo, S., Breton, V., Turbide, C. & Beauchemin, N. *et al.* CEACAM1 deficiency delays important wound healing processes. *Wound Repair. Regen.* **19**, 745–752 (2011).
40. Klaile, E., Klassert, T.E., Scheffrahn, I., Muller, M.M., Heinrich, A. & Heyl, K.A. *et al.* Carcinoembryonic antigen (CEA)-related cell adhesion molecules are co-expressed in the human lung and their expression can be modulated in bronchial epithelial cells by non-typable Haemophilus influenzae, Moraxella catarrhalis, TLR3, and type I and II interferons. *Respir. Res.* **14**, 85 (2013).
41. Sjoelund, V., Smelkinson, M. & Nita-Lazar, A. Phosphoproteome profiling of the macrophage response to different toll-like receptor ligands identifies differences in global phosphorylation dynamics. *J. Proteom. Res.* **13**, 5185–5197 (2014).
42. Mitchell, C., Provost, K., Niu, N., Homer, R. & Cohn, L. IFN- γ acts on the airway epithelium to inhibit local and systemic pathology in allergic airway disease. *J. Immunol.* **187**, 3815–3820 (2011).
43. Negishi, H., Osawa, T., Ogami, K., Ouyang, X., Sakaguchi, S. & Koshiba, R. *et al.* A critical link between Toll-like receptor 3 and type II interferon signaling pathways in antiviral innate immunity. *Proc. Natl Acad. Sci. USA* **105**, 20446–20451 (2008).

44. Gomez, M.I., Lee, A., Reddy, B., Muir, A., Soong, G. & Pitt, A. *et al.* Staphylococcus aureus protein A induces airway epithelial inflammatory responses by activating TNFR1. *Nat. Med.* **10**, 842–848 (2004).
45. Aneja, R.K., Tsung, A., Sjodin, H., Geffer, J.V., Delude, R.L. & Billiar, T.R. *et al.* Preconditioning with high mobility group box 1 (HMGB1) induces lipopolysaccharide (LPS) tolerance. *J. Leukoc. Biol.* **84**, 1326–1334 (2008).
46. Hippenstiel, S., Opitz, B., Schmeck, B. & Suttrop, N. Lung epithelium as a sentinel and effector system in pneumonia—molecular mechanisms of pathogen recognition and signal transduction. *Respir. Res.* **7**, 97 (2006).
47. Mizgerd, J.P. Respiratory infection and the impact of pulmonary immunity on lung health and disease. *Am. J. Respir. Crit. Care Med.* **186**, 824–829 (2012).
48. McClure, R. & Massari, P. TLR-dependent human mucosal epithelial cell responses to microbial pathogens. *Front. Immunol.* **5**, 386 (2014).
49. Yuana, Y., Sturk, A. & Nieuwland, R. Extracellular vesicles in physiological and pathological conditions. *Blood Rev.* **27**, 31–39 (2013).
50. Robbins, P.D. & Morelli, A.E. Regulation of immune responses by extracellular vesicles. *Nat. Rev. Immunol.* **14**, 195–208 (2014).
51. Deeb, R.S., Walters, M.S., Strulovici-Barel, Y., Chen, Q., Gross, S.S. & Crystal, R.G. Smoking-associated disordering of the airway basal stem/progenitor cell metatype. *Am. J. Respir. Cell Mol. Biol.* **54**, 231–240 (2016).
52. Zhao, Y., Jamaluddin, M., Zhang, Y., Sun, H., Ivanciuc, T. & Garofalo, R.P. *et al.* Systematic analysis of cell-type differences in the epithelial secretome reveals insights into the pathogenesis of respiratory syncytial virus-induced lower respiratory tract infections. *J. Immunol.* **198**, 3345–3364 (2017).
53. Grassme, H., Henry, B., Ziobro, R., Becker, K.A., Riethmuller, J. & Gardner, A. *et al.* beta1-Integrin accumulates in cystic fibrosis luminal airway epithelial membranes and decreases sphingosine, promoting bacterial infections. *Cell Host Microbe* **21**, 707–718 e708 (2017).
54. Slevogt, H., Zabel, S., Opitz, B., Hocke, A., Eitel, J. & N'Guessan, P.D. *et al.* CEACAM1 inhibits Toll-like receptor 2-triggered antibacterial responses of human pulmonary epithelial cells. *Nat. Immunol.* **9**, 1270–1278 (2008).
55. Pezzulo, A.A., Starner, T.D., Scheetz, T.E., Traver, G.L., Tilley, A.E. & Harvey, B.G. *et al.* The air-liquid interface and use of primary cell cultures are important to recapitulate the transcriptional profile of in vivo airway epithelia. *Am. J. Physiol. Lung Cell Mol. Physiol.* **300**, L25–L31 (2011).
56. Brown, K.J., Seol, H., Pillai, D.K., Sankoorikal, B.J., Formolo, C.A. & Mac, J. *et al.* The human secretome atlas initiative: implications in health and disease conditions. *Biochim. Biophys. Acta* **1834**, 2454–2461 (2013).
57. Pillai, D.K., Sankoorikal, B.J., Johnson, E., Seneviratne, A.N., Zurko, J. & Brown, K. J. *et al.* Directional secretomes reflect polarity-specific functions in an in vitro model of human bronchial epithelium. *Am. J. Respir. Cell Mol. Biol.* **50**, 292–300 (2014).
58. Nguyen, E.V., Gharib, S.A., Palazzo, S.J., Chow, Y.H., Goodlett, D.R. & Schnapp, L.M. Proteomic profiling of bronchoalveolar lavage fluid in critically ill patients with ventilator-associated pneumonia. *PLoS ONE* **8**, e58782 (2013).
59. Martinez-Anton, A., Sokolowska, M., Kern, S., Davis, A.S., Alsaaty, S. & Taubenberger, J.K. *et al.* Changes in microRNA and mRNA expression with differentiation of human bronchial epithelial cells. *Am. J. Respir. Cell Mol. Biol.* **49**, 384–395 (2013).
60. Heyl, K.A., Klassert, T.E., Heinrich, A., Muller, M.M., Klaile, E. & Dienemann, H. *et al.* Dectin-1 is expressed in human lung and mediates the proinflammatory immune response to nontypeable Haemophilus influenzae. *MBio* **5**, e01492–e01514 (2014).
61. Masuda, T., Tomita, M. & Ishihama, Y. Phase transfer surfactant-aided trypsin digestion for membrane proteome analysis. *J. Proteom. Res.* **7**, 731–740 (2008).
62. Leon, I.R., Schwammle, V., Jensen, O.N. & Sprenger, R.R. Quantitative assessment of in-solution digestion efficiency identifies optimal protocols for unbiased protein analysis. *Mol Cell Proteomics* **12**, 2992–3005 (2013).
63. Grossmann, J., Roschitzki, B., Panse, C., Fortes, C., Barkow-Oesterreicher, S. & Rutishauser, D. *et al.* Implementation and evaluation of relative and absolute quantification in shotgun proteomics with label-free methods. *J Proteomics* **73**, 1740–1746 (2010).
64. Love, M.I., Huber, W. & Anders, S. Moderated estimation of fold change and dispersion for RNA-seq data with DESeq2. *Genome Biol.* **15**, 550 (2014).
65. Murtagh, F.L.P. Ward's hierarchical agglomerative clustering method: which algorithms implement ward's criterion?. *J. Classif.* **31**, 274–295 (2014).
66. Pfaffl, M.W. A new mathematical model for relative quantification in real-time RT-PCR. *Nucleic Acids Res.* **29**, e45 (2001).